PHYSICAL REVIEW B **90**, 220303(R) (2014)

# Interplay of electron heating and saturable absorption in ultrafast extreme ultraviolet transmission of condensed matter

Andrea Di Cicco,[1] Keisuke Hatada,[2,1] Erika Giangrisostomi,[3] Roberto Gunnella,[1] Filippo Bencivenga,[3] Emiliano Principi,[3] Claudio Masciovecchio,[3] and Adriano Filipponi[4]

[1]*Physics Division, School of Science and Technology, Università di Camerino, via Madonna delle Carceri 9, I-62032 Camerino (MC), Italy*
[2]*Département Matériaux-Nanosciences, Institut de Physique de Rennes, UMR CNRS-UR1 6251, Université de Rennes-1, 35042 Rennes cedex, France*
[3]*Synchrotron ELETTRA, Strada Statale 14, I-34149 Basovizza, Trieste, Italy*
[4]*Dipartimento di Scienze Fisiche e Chimiche, Università degli Studi dell'Aquila, I-67100 L'Aquila, Italy*

(Received 8 September 2014; revised manuscript received 10 November 2014; published 15 December 2014)

High intensity pulses obtained by modern extreme ultraviolet (EUV) and x-ray photon sources allows the observation of peculiar phenomena in condensed matter. Experiments performed at the Fermi@Elettra FEL-1 free-electron-laser source at 23.7, 33.5, and 37.5 eV on Al thin films, for an intermediate-fluence range up to about 20 J/cm$^2$, show evidence for a nonmonotonic EUV transmission trend. A decreasing transmission up to about 5–10 J/cm$^2$ is followed by an increase at higher fluence, associated with saturable absorption effects. The present findings are interpreted within a simplified three-channel model, showing that an account of the interplay between ultrafast electron heating and saturation effects is required to explain the observed transmission trend.

DOI: 10.1103/PhysRevB.90.220303 PACS number(s): 78.70.Dm, 78.40.Kc, 78.66.Bz

Novel extreme ultraviolet (EUV) and x-ray sources delivering intense and ultrashort photon pulses [1–4] are able to induce extremely interesting photon-matter interaction processes which are usually neglected. In particular, saturable absorption effects and high levels of deposited energy (ultrafast electron heating) are both phenomena that are expected to affect the opacity of materials [5,6]. Nowadays, free-electron-laser (FEL) facilities allow us to reach unprecedented levels of fluence per photon pulse. Deviations from the typical well-known exponential decay (Lambert-Beer law), valid for both extreme ultraviolet (EUV) and x-ray photons under moderate flux conditions, are thus expected.

Saturable absorption inducing increased transparency of materials was observed in transmission measurements above the $L_{II,III}$ edge of pure Al thin films using ultrashort FEL soft x-ray pulses [5], in ultrathin Sn films using EUV FEL radiation [6,7], and more recently at higher photon energy in iron [8]. The high intensity reachable by FEL pulses, the shortness of the pulse duration, and the typical lifetime of the excited state are all important factors enabling observation of the phenomenon. The results of Nagler *et al.* [5] were obtained using subpicosecond soft x-ray pulses (92 eV photon energy) with intensities up to and in excess of $10^{16}$ W cm$^{-2}$ (fluences up to $\sim$200 J/cm$^2$ for each pulse). In that experiment, large deposited energies in the ultrathin Al foil allowed the creation of highly uniform warm dense matter (WDM) conditions [9,10], a regime exceedingly difficult to reach in laboratory studies, but of great interest in various fields, including high-pressure and planetary science, astrophysics, and plasma production. As a matter of fact, warm dense matter at electron temperatures in the 1–10 eV range can be generated by EUV and x-ray FEL radiation [10–13], and various ultrafast techniques can be used to probe WDM properties in that regime.

Those previous results naturally call for further challenging experiments and the development of suitable interpretation schemes for modeling and understanding the EUV/x-ray absorption cross section under high-fluence conditions. The present availability of tunable FEL radiation in the ultraviolet (UV) and soft x-ray ranges such as Flash (Hamburg) [1] and Fermi@Elettra (Trieste) [3,14] and in the hard x-ray range such as LCLS (Stanford) [2], SACLA (Spring-8) [4], and of the future European XFEL (presently under construction) gives us an extraordinary experimental opportunity [15] for probing the properties of dense matter under extreme conditions.

In this Rapid Communication, we report the results of EUV transmission experiments on Al thin films, measured in an intermediate range of fluence. Results are interpreted in the framework of a simplified theoretical approach accounting for saturation and electron heating effects. The purpose of this work is thus twofold, as it provides both EUV experimental data and modeling of the variation of the fluence-dependent transmission in condensed matter.

The EUV transmission experiments have been performed at the TIMEX end station [16–18] of the Elastic and Inelastic Scattering (EIS) beamline, using the FERMI@Elettra FEL-1 source, a seeded FEL providing clean, tunable [3,14], and intense subpicosecond [100 fs full width at half maximum (FWHM)] photon pulses in the 19–62 eV photon energy range. In Fig. 1 we show the TIMEX [16–19] experimental setup used for the present experiments including important details of the photon transport and diagnostics systems. Diagnostics and intensity tuning of the FEL pulses are provided through a dedicated system (PADReS [3,14,20]), including a spectrometer for measuring the pulse shape. As shown in the right hand side of Fig. 1, a gas attenuation chamber allows for adjustments of the FEL pulse intensity, while two low-pressure ionization chambers placed before and after the gas chamber are calibrated to provide measurements of the intensity ($I_0$) at the FEL exit for each individual pulse. A 200 nm flat Al filter is available within the (unfocused) FEL beam transport section to eliminate the seed laser contribution. Different experimental stations can be selected by controlling a switching mirror.

The sample-photon interaction region is located inside the TIMEX chamber, including a five-axis motorized manipulator holding samples and pulse diagnostics, the detector for transmitted intensity $I_1$, the focusing mirror, and the telemicroscope

 

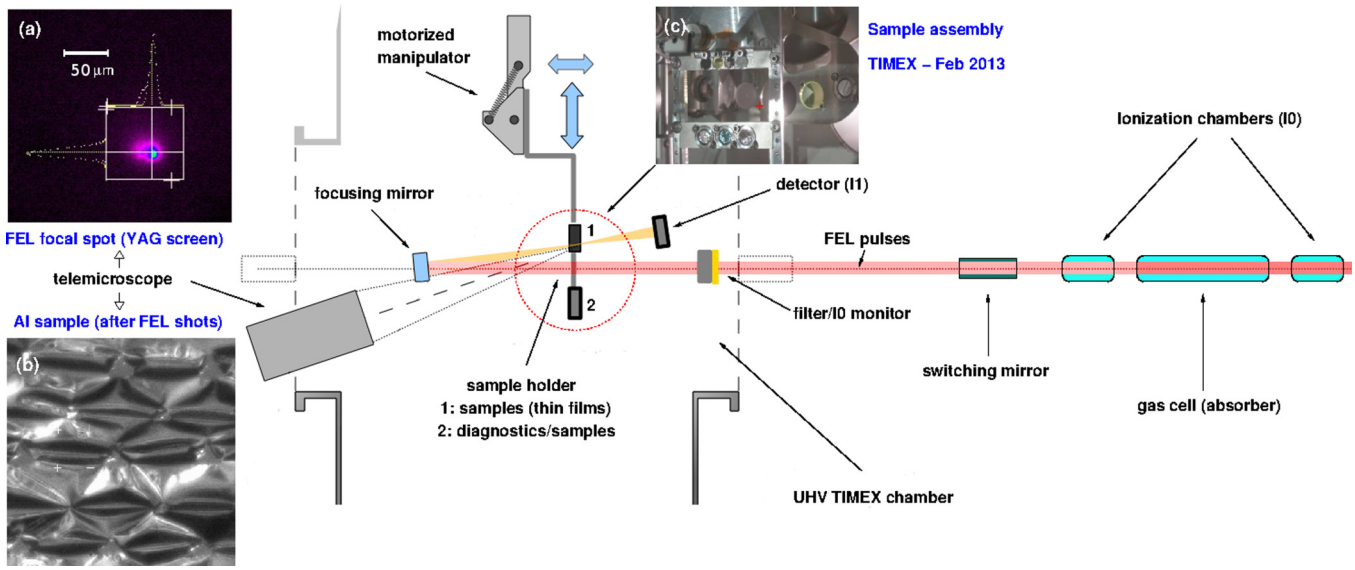


FIG. 1. (Color online) Sketch of the experimental setup including optics, diagnostics, and detectors for the transfer and control of the FEL pulses generated by the Fermi@Elettra FEL-1 source (right, not shown). From the right to the left (main figure) FEL pulses pass through ionization chambers (measuring the intensity $I_0$), a gas cell absorber (fluence reduction), a plane mirror, and selected filters. On the left side we show the setup inside the UHV TIMEX chamber: the motorized manipulator holding sample and pulse diagnostics, the detector (photodiode measuring $I_1$), the focusing mirror, and the telemicroscope. (a) The FEL focal spot at sample position; (b) an image of the Al ultrathin sample surface after FEL pulse exposures; (c) the multisample assembly for this experiment.

for centering the beam on the sample (see the center of Fig. 1). Focusing of the beam has been provided by a spherical platinum-coated silicon mirror (400 mm radius of curvature, 0.2 nm roughness rms) placed close to normal incidence (angle of incidence 3°), which is able to provide a focal spot of area $\sigma^2 \approx 100\ \mu\text{m}^2$. The maximum energy per pulse delivered by the FEL source for the present experiment has been in the 300, 180, and 130 $\mu$J range at 23.7, 33.3, and 37 eV photon energy, respectively. Data were collected over two to three decades of incoming fluence $F$ through the combined use of filters and the gas attenuator. Appreciable damages to the sample surface were observed after irradiation with a single FEL pulse with $F > 0.1\ \text{J/cm}^2$. Each individual shot has been tagged by a unique label (bunch number) allowing single-shot transmittance measurements. The actual incoming fluence $F$ on the sample was determined by taking into account the area of the focal spot ($\sigma^2$) as well as the mirror reflectivity and beamline transmission. The detector for the transmitted photon intensity $I_1$ was a silicon photodiode (UVG20S, IRD, Inc.) coupled with a 0.5 mm thick YAG fluorescence screen having a 100 nm aluminum coating on the FEL side. Samples for the present experiments have been unsupported self-standing 100 nm thick Al foils, mounted on UHV-compatible 10 mm rings (Lebow Co., Goleta, CA).

The FEL focal spot at sample position, shown in Fig. 1(a), was refined using a YAG screen located on the multisample assembly [Fig. 1(c)] of the manipulator. The best lateral dimension of the pulse at focus was found to be $\sim$10 $\mu$m (FWHM). The telemicroscope (Questar QM-100) has been used both to determine the *in situ* size and shape of the FEL spot as well as the status of the samples in the interaction region. The effect of exposition to the FEL pulses on the samples can be appreciated by looking at Fig. 1(b). The motorized sample manipulator stage is conceived for single-shot measurements at a 10–100 Hz rate and has allowed positioning of each FEL pulse on undamaged sample regions. In the present experiment, we have collected a large set of transmission data for repeated FEL shots moving the Al target in new positions for each shot.

The set of postprocessed transmission measurements ($T = I_1/I_0$) collected at three different photon energies in a wide range of incoming fluence is reported in Fig. 2. Due to the limited efficiency of the optics (using a mirror at normal incidence), the maximal fluence reached has been $\approx$20, 13, and 10 J/cm$^2$ at 23.7, 33.3, and 37 eV photon energy, respectively. Single-shot measurements are individually presented in Fig. 2, as a result of different experimental campaigns varying the FEL photon wavelength, using the natural intensity fluctuations of the FEL pulses, the pressure of the gas absorber, and the presence of filters. Extended calibration curves of the $I_1$ signal with respect to $I_0$ measured by the ionization chambers were collected prior to each measurement in the entire range of fluence available. The thickness homogeneity of the Al thin films was estimated to be within 5%, as indicated by prolonged collections of transmission data with FEL pulses below the damage limits. The random noise on single-shot transmission data is due to a combination of counting statistics and thickness fluctuations. The observed transmission is reproducible over successive fluence sweeps, and the solid curves reported in Fig. 2 refer to the confidence interval for single-shot measurements obtained from the average and standard deviation of data point subsamples over successive fluence intervals. The transmission variation with $F$ is statistically significant. At low photon energy (23.7 eV) the high absorption of Al and the low efficiency of the detector did not allow us to collect reliable low-fluence measurements

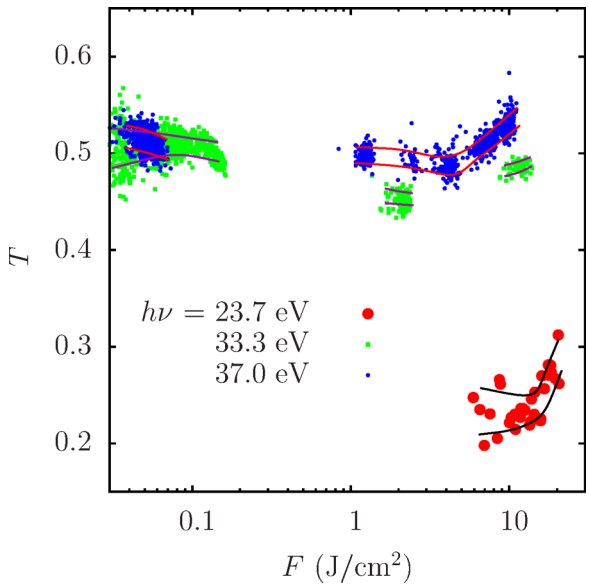


FIG. 2. (Color online) Single-shot transmission data of FEL-1 pulses across an ultrathin 100 nm Al foil as a function of the estimated fluence $F$. Data refer to a FEL photon energy of 23.7 eV (red circles), 33.3 eV (green squares), and 37.0 eV (blue circles). Lines depicted for each photon energy enclose bands of estimated uncertainty (standard deviation) for the single-shot data points within successive $F$ intervals.

(below $F = 5$ J/cm$^2$). The other two sets of measurements (33.3 and 37 eV) are instead presented over three decades of incoming fluence $F$ (0.01 to $\sim$10 J/cm$^2$).

Looking at Fig. 2 we can notice that the observed trend of transmittance for increasing incoming fluence includes a decrease at intermediate fluence ($F < 5$ J/cm$^2$) followed by an increase for higher-fluence levels. This trend is clearly visible at 33.3 and 37.0 eV, while the quality of the data at 23.7 eV allows only observation of the increased transmittance at high fluence. The increased transmission is qualitatively similar to the one previously measured at higher photon energy [5], but a full understanding of the observed trend is required for the development of suitable models and computational tools.

In a recent work [21], we developed a phenomenological three-state model which is able to reproduce saturation phenomena related to the increased transmission. We refer to the original publication [21] for more details on the computational model. In brief, the model describes the variation of the density of occupation numbers $N_1$, $N_2$, and $N_3$ of the three many-body states (ground $|1\rangle$, excited $|2\rangle$, and an intermediate relaxed state $|3\rangle$) by a set of rate equations with proper constraints:

$$\begin{aligned}
\frac{dN_1(z,t)}{dt} &= \frac{g(z,t)I(z,t)}{h\nu} + \frac{N_2(z,t)}{\tau_{21}} + \frac{N_3(z,t)}{\tau_{31}},\\
\frac{dN_2(z,t)}{dt} &= -\frac{g(z,t)I(z,t)}{h\nu} - \frac{N_2(z,t)}{\tau_{21}} - \frac{N_2(z,t)}{\tau_{23}},\\
\frac{dN_3(z,t)}{dt} &= \frac{1}{\tau_{23}}N_2(z,t) - \frac{1}{\tau_{31}}N_3(z,t),\\
g(z,t) &= \sigma(T)[N_2(z,t) - N_1(z,t)],\\
N &= N_1(z,t) + N_2(z,t) + N_3(z,t).
\end{aligned} \tag{1}$$

In this set of equations, the occupation numbers depend thus on the photon field intensity $I(z,t)$ at time $t$ and position $z$ (along the direction of propagation of the pulse), the photon absorption cross section $\sigma$ at given photon energy $\hbar\omega$, and on the relaxation times $\tau$ between the various states. In this formalism, $g(z,t)$ is an effective time- and space-dependent absorption coefficient, possibly temperature dependent, that can be considered to be constant for linear absorption (Lambert-Beer law).

Equations (1) are coupled with the transport condition of the incoming pulse, within the classical electrodynamics limit,

$$\frac{dI(z,t)}{dz} + \frac{1}{c}\frac{dI(z,t)}{dt} = g(z,t)I(z,t). \tag{2}$$

Within the model described by Eqs. (1) and (2), absorption and stimulated emission by laser radiation involve transitions between ground $|1\rangle$ and excited $|2\rangle$ states. The relaxed state $|3\rangle$ represents the ensemble of all possible relaxed states reached by decay of state $|2\rangle$. It can decay to state $|1\rangle$ by emitting a photon or through other processes.

Equations can be solved numerically following the dynamics of the pulse, using discretized grids with $\Delta t = 0.4$ as and $\Delta z = 1.2$ nm which satisfy the *Courant condition*, $c \leqslant \Delta z/\Delta t$, so that the "upward differencing" method can be applied safely [22]. Application of Eqs. (1) and (2) within a suitable computational scheme has been shown to explain previous experiments on saturable absorption [21].

In the present experiment, the decrease of EUV transmission observed in an intermediate range of fluence (see Fig. 2) cannot be simply described by the rate equations, and we need to include explicitly the increase of electron temperature in the model. Detailed calculations of the temperature dependence of the EUV absorption coefficient of aluminum are reported in a recent paper [23], showing a peculiar increase of absorption in an intermediate range of electron temperatures (1–10 eV).

We have included the temperature dependence in our model for EUV transmission by calculating the deposited energy $E_{\rm abs}$ through the Al thin film, and using the Maxwell-Boltzmann approximation for the electron temperature $T_e$: $\langle E\rangle = \frac{3}{2}k_B\langle T\rangle$. Within this approach, the temperature variation $\Delta T_e$ for each slice $\Delta z$ of a thin film of given valence electron density $n_e$ is simply related to the fluence change $\Delta F$ (deposited energy per unit surface): $k_B\Delta T_e = \frac{2}{3n_e}\frac{\Delta F}{\Delta z}$. The temperature dependence of the absorption cross section $[\sigma(T)]$ has been then calculated on the basis of previous WDM calculations [23] as a result of the deposited energy ($\Delta F$) in each slice and Eqs. (1) and (2) solved numerically.

For free-free EUV absorption, the effective lifetime of the excited state can be much longer than that of excited core levels ($\sim$40 fs for $L_{\rm II,III}$ edge [24]) due to the presence of complex thermalization processes involving filling a hole in a valence state, transport of electrons, and Auger recombination [25]. Those processes and the naturally long lifetime of Fermi-liquid states near $E_F$ can lead to thermalization times in excess of 400 fs [25]. Based on these considerations, the FEL pulse width ($\tau_{\rm FEL} = 100$ fs) has been considered to be shorter than the lifetimes of the excited states $\tau_{21}, \tau_{31}$. We have verified that EUV transmission curves as a function of fluence are

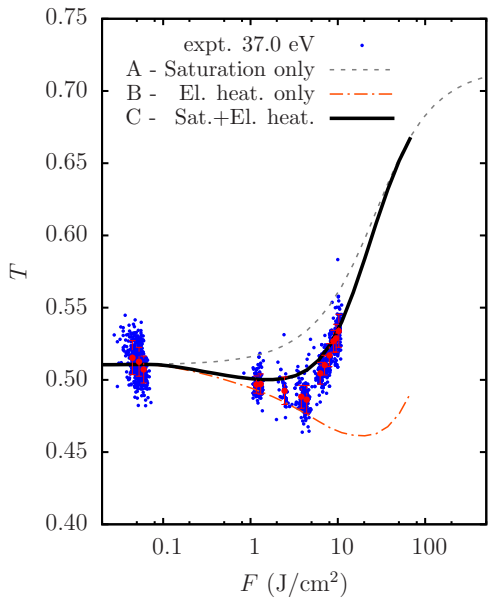


FIG. 3. (Color online) Experimental EUV transmission data compared with different calculations (see text). Curve *A* includes only optical saturation phenomena without accounting for temperature effects; curve *B* includes electron heating but neglects saturation phenomena; curve *C* takes into account both electron heating and saturation effects. The vertical bars refer to the average and standard deviations of single-shot data points within successive *F* intervals.

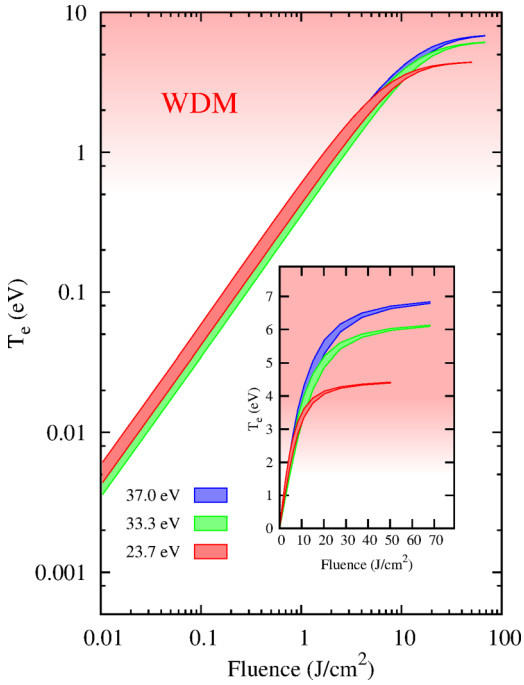


FIG. 4. (Color online) Estimated electron temperature in the 100 nm thick Al thin film as a function of incoming fluence at different FEL photon energies (curves enclose maximal and minimal temperatures through the film for given fluence). Electron temperatures in excess of 1 eV are obtained for fluence regimes above $\sim$3 J/cm$^2$. Saturable absorption is found to limit the deposited energy above 10 J/cm$^2$ providing uniform bulk heating in the high-fluence regime (see the inset on a linear scale).

practically insensitive to the precise value of those lifetimes in the range 0.2–1 ps ($\tau_{21} = \tau_{31} = 500$ fs was used for the final calculations). On the other hand, the typical decay time $\tau_{23}$ to the intermediate state was estimated from the inelastic mean free path curve ($\tau_{23} \sim 1$ fs at 20 eV of electron kinetic energy).

The results of our calculations are compared with EUV transmission experiments in Fig. 3. Three different model calculations have been performed: including only optical saturation phenomena (curve *A*); considering only electron heating but neglecting saturation phenomena (curve *B*); and including both electron heating and saturation effects (curve *C*). As shown in Fig. 3, model *A* is not able to account for the decrease observed in EUV transmission as expected. Model *B* accounts only for the temperature change in the absorption cross section $\sigma(T)$ and overestimates the EUV transmission decrease. Model *C*, including both electron heating and saturation phenomena, reproduces the essential features of the EUV transmission trend.

The computational model allows us also to estimate the electron temperature throughout the film. In Fig. 4 we report the curves enclosing the minimal and maximal electron temperature reached within the film as a function of the FEL pulse incoming fluence (at 23.7, 33.3, and 37 eV photon energy). Electron temperatures $k_B T_e$ in excess of 1 eV are obtained for fluence regimes above $F \sim 3$ J/cm$^2$. An almost linear trend (see also Ref. [19]) and a spread of electron temperatures (up to about 15%) is obtained through the thin Al film, up to fluence regimes in the 10 J/cm$^2$ range. Saturable absorption is found to limit the deposited energy for $F > 10$ J/cm$^2$ providing quasiuniform bulk heating in the high-fluence regime (up to $T_e \sim 7$ eV for 37 eV photons).

In conclusion, here we have reported the results of EUV transmission experiments on Al thin films in the 20–40 eV photon energy range for fluences up to about 20 J/cm$^2$. We show that transmission is first decreasing, as an effect of ultrafast electron heating, and then increasing, mostly as an effect of saturation. The results are interpreted in the framework of a simplified theoretical approach accounting for the two effects, both necessary to explain the experimental observations. The present data and simulations indicate that electron temperatures in excess of 1 eV are obtained in single-shot EUV transmission experiments at fluences larger than 3 J/cm$^2$.

This work has been carried out in the framework of the TIMEX collaboration (time-resolved studies of matter under extreme and metastable conditions: http://gnxas.unicam.it/TIMEX), aimed to develop an end station at the FERMI@Elettra FEL facility in Trieste. TIMEX is a project financed by the ELETTRA synchrotron radiation facility in Trieste in collaboration with the University of Camerino. K.H. gratefully acknowledges TIMEX research grants for support. A.D.C., R.G., and K.H. acknowledge the COST Action MP1306 EUSpec and the European FP7 MSNano network under Grant Agreement No. PIRSES-GA-2012-317554.

[1] W. Ackermann, G. Asova, V. Ayvazyan, A. Azima, N. Baboi, J. Bähr, V. Balandin, B. Beutner, A. Brandt, A. Bolzmann *et al.*, Nat. Photonics **1**, 336 (2007).

[2] P. Emma, R. Akre, J. Arthur, R. Bionta, C. Bostedt, J. Bozek, A. Brachmann, P. Bucksbaum, R. Coffee, F.-J. Decker *et al.*, Nat. Photonics **4**, 641 (2010).

[3] E. Allaria, R. Appio, L. Badano, W. A. Barletta, S. Bassanese, S. G. Biedron, A. Borga, E. Busetto, D. Castronovo, P. Cinquegrana *et al.*, Nat. Photonics **6**, 699 (2012).

[4] T. Ishikawa, H. Aoyagi, T. Asaka, Y. Asano, N. Azumi, T. Bizen, H. Ego, K. Fukami, T. Fukui, Y. Furukawa *et al.*, Nat. Photonics **6**, 540 (2012).

[5] B. Nagler, U. Zastrau, R. R. Fustlin, S. M. Vinko, T. Whitcher, A. J. Nelson, R. Sobierajski, J. Krzywinski, J. Chalupsky, E. Abreu *et al.*, Nat. Phys. **5**, 693 (2009).

[6] H. Yoneda, Y. Inubushi, T. Tanaka, Y. Yamaguchi, F. Sato, S. Morimoto, T. Kumagai, M. Nagasono, A. Higashiya, M. Yabashi, T. Ishikawa, H. Ohashi, H. Kimura, H. Kitamura, and R. Kodama, Opt. Express **17**, 23443 (2009).

[7] Y. Inubushi, H. Yoneda, A. Higashiya, T. Ishikawa, H. Kimura, T. Kumagai, S. Morimoto, M. Nagasono, H. Ohashi, F. Sato, T. Tanaka, T. Togashi, K. Tono, M. Yabashi, Y. Yamaguchi, and R. Kodama, Rev. Sci. Instrum. **81**, 036101 (2010).

[8] H. Yoneda, Y. Inubushi, M. Yabashi, T. Katayama, T. Ishikawa, H. Ohashi, H. Yumoto, K. Yamauchi, H. Mimura, and H. Kitamura, Nat. Commun. **5**, 5080 (2014).

[9] R. W. Lee, S. J. Moon, H.-K. Chung, W. Rozmus, H. A. Baldis, G. Gregori, R. C. Cauble, O. L. Landen, J. S. Wark, A. Ng, S. J. Rose, C. L. Lewis, D. Riley, J.-C. Gauthier, and P. Audebert, J. Opt. Soc. Am. B **20**, 770 (2003).

[10] A. Krenz and J. Meyer-ter-Vehn, J. Phys. IV (France) **133**, 1097 (2006).

[11] U. Zastrau, C. Fortmann, R. R. Fäustlin, L. F. Cao, T. Döppner, S. Düsterer, S. H. Glenzer, G. Gregori, T. Laarmann, H. J. Lee *et al.*, Phys. Rev. E **78**, 066406 (2008).

[12] A. Lévy, F. Dorchies, M. Harmand, C. Fourment, S. Hulin, O. Peyrusse, J. J. Santos, P. Antici, P. Audebert, J. Fuchs, L. Lancia, A. Mancic, M. Nakatsutsumi, S. Mazevet, V. Recoules, P. Renaudin, and S. Fourmaux, Plasma Phys. Controlled Fusion **101**, 15002 (2009).

[13] S. H. Glenzer and R. Redmer, Rev. Mod. Phys. **81**, 1625 (2009).

[14] E. Allaria, A. Battistoni, F. Bencivenga, R. Borghes, C. Callegari, F. Capotondi, D. Castronovo, P. Cinquegrana, D. Cocco, M. Coreno *et al.*, New J. Phys. **14**, 113009 (2012).

[15] F. Rosmej, R. Lee, D. Riley, J. M. ter Vehn, A. Krenz, T. Tschentscher, A. Tauschwitz, A. Tauschwitz, V. Lisitsa, and A. Faenov, J. Phys.: Conf. Ser. **72**, 12007 (2007).

[16] A. Di Cicco, F. D'Amico, G. Zgrablic, E. Principi, R. Gunnella, F. Bencivenga, C. Svetina, C. Masciovecchio, F. Parmigiani, and A. Filipponi, J. Non-Cryst. Solids **357**, 2641 (2011).

[17] A. Di Cicco, F. Bencivenga, A. Battistoni, D. Cocco, R. Cucini, F. D'Amico, S. D. Fonzo, A. Filipponi, A. Gessini, E. Giangrisostomi, R. Gunnella, C. Masciovecchio, E. Principi, and C. Svetina, Proc. SPIE **8077**, 807704 (2011).

[18] A. Di Cicco, C. Masciovecchio, F. Bencivenga, E. Principi, E. Giangrisostomi, A. Battistoni, R. Cucini, F. D'Amico, S. Di Fonzo, A. Gessini, K. Hatada, R. Gunnella, and A. Filipponi, Notiziario Neutroni e Luce di Sincrotrone **18**, 19 (2013).

[19] F. Bencivenga, E. Principi, E. Giangrisostomi, R. Cucini, A. Battistoni, F. D'Amico, A. Di Cicco, S. Di Fonzo, A. Filipponi, A. Gessini, R. Gunnella, M. Marsi, L. Properzi, M. Saito, and C. Masciovecchio, Sci. Rep. **4**, 4952 (2014).

[20] D. Cocco, A. Abrami, A. Bianco, I. Cudin, C. Fava, D. Giuressi, R. Godnig, F. Parmigiani, L. Rumiz, R. Sergo, C. Svetina, and M. Zangrando. Proc. SPIE **7361**, 736106 (2009).

[21] K. Hatada and A. Di Cicco, J. Electron Spectrosc. Relat. Phenom. **196**, 177 (2014).

[22] R. Courant, K. Friedrichs, and Lewy, IBM J. Res. Dev. **11**, 215 (1967).

[23] S. M. Vinko, G. Gregori, M. P. Desjarlais, B. Nagler, T. J. Whitcher, R. W. Lee, P. Audebert, and J. S. Wark, High Energy Density Phys. **5**, 124 (2009).

[24] C.-O. Almbladh, A. L. Morales, and G. Grossmann, Phys. Rev. B **39**, 3489 (1989).

[25] N. Medvedev, U. Zastrau, E. Förster, D. O. Gericke, and B. Rethfeld, Phys. Rev. Lett. **107**, 165003 (2011).